

Wide Dispersion and Diversity of Clonally Related Inhibitory Interneurons

Highlights

- Cortical interneurons derive from symmetric divisions of intermediate progenitors
- Histologically distinct interneuron subtypes derive from the same clonal lineage
- Clonally related interneurons are widely dispersed

Authors

Corey C. Harwell, Luis C. Fuentealba, Adrian Gonzalez-Cerrillo, ..., Arturo Alvarez-Buylla, Constance L. Cepko, Arnold R. Kriegstein

Correspondence

corey_harwell@hms.harvard.edu

In Brief

The mechanisms that guide the diversity and organization of GABAergic interneurons are not well understood. Harwell et al. show that interneurons derived from the same clonal lineage are composed of diverse subtypes that are widely dispersed throughout the forebrain.



Wide Dispersion and Diversity of Clonally Related Inhibitory Interneurons

Corey C. Harwell,^{1,*} Luis C. Fuentealba,^{2,5} Adrian Gonzalez-Cerrillo,¹ Phillip R.L. Parker,⁴ Caitlyn C. Gertz,^{3,5} Emanuele Mazzola,⁶ Miguel Turrero Garcia,¹ Arturo Alvarez-Buylla,^{2,5} Constance L. Cepko,⁷ and Arnold R. Kriegstein^{3,5}

¹Department of Neurobiology, Harvard Medical School, Boston, MA 02115, USA

²Department of Neurological Surgery

³Department of Neurology

University of California, San Francisco, San Francisco, CA 94143, USA

⁴Gladstone Institute for Neurological Disease, San Francisco, CA 94158, USA

⁵Eli and Edythe Broad Center of Regeneration Medicine and Stem Cell Research, San Francisco, CA 94143, USA

⁶Department of Biostatistics, Harvard School of Public Health, Boston, MA 02115, USA

⁷Departments of Genetics and Ophthalmology and Howard Hughes Medical Institute, Harvard Medical School, Boston, MA 02115, USA

*Correspondence: corey_harwell@hms.harvard.edu

<http://dx.doi.org/10.1016/j.neuron.2015.07.030>

SUMMARY

The mammalian neocortex is composed of two major neuronal cell types with distinct origins: excitatory pyramidal neurons and inhibitory interneurons, generated in dorsal and ventral progenitor zones of the embryonic telencephalon, respectively. Thus, inhibitory neurons migrate relatively long distances to reach their destination in the developing forebrain. The role of lineage in the organization and circuitry of interneurons is still not well understood. Utilizing a combination of genetics, retroviral fate mapping, and lineage-specific retroviral barcode labeling, we find that clonally related interneurons can be widely dispersed while unrelated interneurons can be closely clustered. These data suggest that migratory mechanisms related to the clustering of interneurons occur largely independent of their clonal origin.

INTRODUCTION

The cerebral cortex is one of the most intricate structures in the mammalian nervous system and is responsible for complex behaviors associated with cognitive function. Nearly all cortical neurons are produced during a limited time window of cortical neurogenesis that occurs during embryonic development (Miller and Gauthier, 2007). In the dorsal telencephalon, radial glia (RG) that line the lateral ventricles and outer RG (oRG) that reside in the subventricular zone divide asymmetrically to produce intermediate progenitor cells (IPCs) and neurons (Hansen et al., 2010; Noctor et al., 2001, 2004; Wang et al., 2011). In rodents, the IPCs divide symmetrically to produce pairs of excitatory neurons (Haubensak et al., 2004; Noctor et al., 2004). Clonally related excitatory neurons migrate along the scaffold of RG fibers to form radial arrays across cortical layers (Noctor et al., 2001; Rakic, 1988; Vasistha et al., 2014).

Recent work has implicated clonal relationships among excitatory pyramidal neurons in the formation of stereotypical cortical microcircuitry (Yu et al., 2009). In contrast, inhibitory interneurons are produced in the embryonic ventral telencephalon and follow a complex migratory route, including a phase of prolonged tangential migration, in order to populate the cortex and hippocampus, as well as subpallial structures such as the striatum and amygdala (Anderson et al., 2001, 2002; Nery et al., 2002; Tricoire et al., 2011; Wonders and Anderson, 2006). Nearly all GABAergic interneurons in the brain arise in the medial ganglionic eminence (MGE) and caudal ganglionic eminence (CGE) (Butt et al., 2005; Nery et al., 2002; Wonders and Anderson, 2006; Xu et al., 2004). MGE progenitors mostly give rise to two functionally distinct subtypes of interneurons: parvalbumin (PV)-expressing fast spiking interneurons and somatostatin (SOM)-expressing non-fast-spiking interneurons. MGE progenitors are molecularly defined by the expression of the homeodomain transcription factor Nkx2.1, which is required for interneuron migration and specification of mature interneuron identity (Butt et al., 2008; Nóbrega-Pereira et al., 2008). The extrinsic signals involved in regulating the migration and positioning of newborn interneurons have been extensively studied (Marín, 2013). However, the roles of intrinsic determinants, such as clonal lineage, and their possible contribution to the distribution of MGE-derived interneurons remain poorly understood. In this study, we seek to determine the relationship between clonal identity and final position of interneurons by utilizing a retroviral barcode library targeted to infect Nkx2.1-expressing progenitor cells. This approach revealed that single progenitor cells can produce cells of both SOM and PV subtypes, that clonally related interneurons can disperse widely throughout different structural and functional regions of the brain, and that cells from unrelated clones can cluster together with a non-random distribution.

RESULTS

To identify the morphological features and proliferative status of cells in the ventral telencephalon, we performed in utero

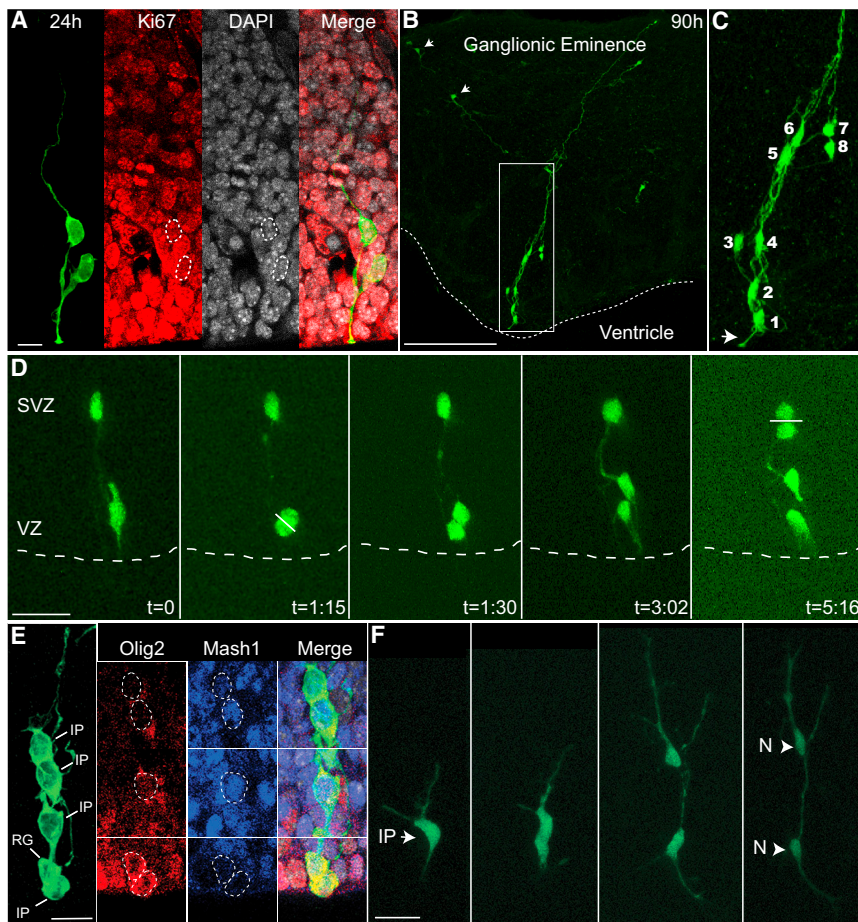


Figure 1. MGE Progenitors Are Arranged in Radial Arrays of Clonally Related Cells

(A) 24 hr after injection we observed a single RG cell and its progeny. Both the RG cell and progeny were positive for the proliferative cell marker Ki67.

(B) Radial arrays of cells in the mouse MGE approximately 90 hr after injection with a GFP-expressing retrovirus. Neurons are also observed migrating tangentially away from the clone (arrowheads).

(C) Higher magnification view of the clone identifies eight anatomically associated cells, one being a RG cell with an apical endfoot (arrowhead) attached to the ventricular surface.

(D) Time-lapse imaging of a RG cell in the MGE shows an asymmetrical RG cell division at the ventricular surface that produces an IPC, and also a previously generated IPC dividing in the SVZ.

(E) Retroviral GFP-labeled MGE progenitors 48 hr after viral infection. Non-RG progeny express bHLH transcription factors Mash1 (blue) and Olig2 (red) $n = 134$.

(F) Time-lapse imaging of an E13.5 embryonic mouse organotypic slice shows a GFP+ IPC dividing to produce a pair of neuronal progeny. Scale bars: (A) 15 μm , (B) 300 μm , (D) 25 μm , and (E) and (F) 20 μm .

The expression of basic helix-loop-helix (bHLH) transcription factors is required for the specification of cortical interneuron progenitors (Petryniak et al., 2007). Therefore, we examined bHLH transcription factor expression in cells located in the SVZ of the MGE 48 hr after in utero infection.

intraventricular retrovirus injections in embryonic mouse brains at gestational day 12.5 (E12.5) (Walantus et al., 2007), coinciding with peak neurogenesis (Butt et al., 2005; Miyoshi et al., 2007). We examined interneuron progenitor cells in the MGE (Anderson et al., 2001) 24–90 hr after infection (Figures 1A–1C). MGE progenitors infected with GFP-expressing retroviruses produced radial clusters of cells similar to those previously observed in the dorsal telencephalon (Noctor et al., 2001). Examination of the MGE 24 hr after injection revealed either single cells or multi-cell clones primarily composed of two cells, typically both Ki67-positive (Figure 1A). Nearly all Ki67-positive cells at this time point were RG or IPCs based upon known morphological features (97%, $n = 4$ brains, 35 cells) (Noctor et al., 2004). At later time points (48–90 hr), clonal clusters consisted of two to eight cells (3.12 ± 1.26 cells per cluster at 48 hr, $n = 49$ clusters) containing one RG cell with a single apical process attached to the ventricular surface, along with several presumptive multipolar IPCs and newborn neurons (Figures 1B and 1C).

To examine the division patterns of these progenitors, we made organotypic slices 24 hr after in utero intraventricular injection of GFP-expressing retrovirus at E12.5 and monitored cell divisions by time-lapse microscopy. We were able to observe nine divisions of MGE cells with RG morphology, and in each imaging session, the RG cell divided at the ventricular surface to produce a presumptive IPC that went on to divide in the SVZ (Figure 1D).

We found that a majority of GFP-positive cells (85%, $n = 3$ brains, 134 cells) coexpressed the ventral telencephalic progenitor markers Olig2 (20.8%), Mash1 (29.9%), or both (34.3%) (Casarosa et al., 1999; Petryniak et al., 2007) (Figures 1E, S1, and S2). We also characterized the pattern of cell division of IPCs in the SVZ of the MGE using time-lapse microscopy (Figure 1F). We observed 13 divisions of SVZ progenitors, each producing two cells with the bipolar morphology of migrating neurons. During one imaging session, we observed SVZ cells undergoing division to produce two daughter cells that each divided again, resulting in four neuronal progeny (Movie S1). This suggests that IPC divisions contribute to the expansion of neuronal lineages in the MGE similar to the way they contribute to neurogenesis in the dorsal telencephalon (Lui et al., 2011; Noctor et al., 2004; Vasistha et al., 2014).

A previous study suggested that clonal relationships might regulate the clustering or distribution of sibling interneurons (Brown et al., 2011). This suggestion raises the possibility that migration of sibling cells may be coordinated. We found that 2–8 hr after birth, pairs of sibling neurons ($n = 8$) rapidly migrated in multiple directions independent of each other (Movie S1), consistent with previous studies reporting that the trajectories of newborn neurons in the MGE mantle zone vary randomly (Tanaka et al., 2009). It was not possible to simultaneously track the movement of sibling cells to their final

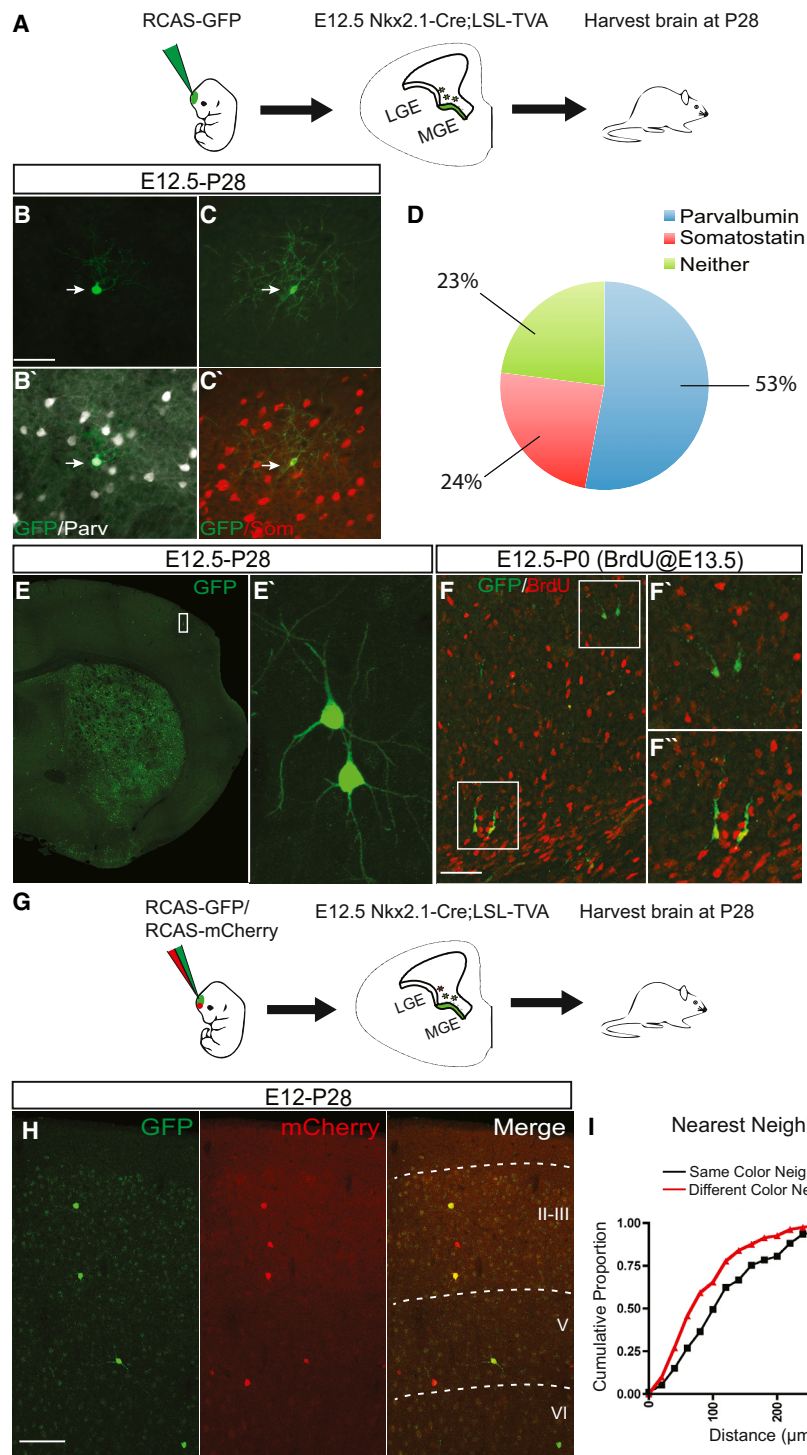


Figure 2. Clustering of Sparsely Labeled MGE Progenitors

(A) E12.5 Nkx2.1-Cre;LSL-Tva mouse embryo showing the TVA⁺ region of the MGE progenitor zone where RCAS viral infection is permitted, in green.

(B–C') P28 brain sections containing RCAS-GFP virus-labeled clones stained with PV (white) ([B] and [B']) or SOM (red) ([C] and [C']).

(D) Pie chart showing the percentage of cells positive for PV, SOM, or negative for both markers (Neither) from Nkx2.1-Cre;LSL-Tva-injected brains (n = 4 brains, 701 cells).

(E) Coronal section of P28 mouse brain injected with RCAS-EGFP virus at E12.5. Sparse EGFP⁺ neurons appear to cluster together into groups of two or more cells in the cortex.

(F) RCAS-EGFP-labeled neurons, derived from infections of progenitors in the developing cortex with a BrdU pulse given 24 hr after infection (red), showing that EGFP⁺ neighboring cells often share the same BrdU labeling status. The upper box shows a pair of BrdU[−] migratory neurons (upper magnified panel F'), whereas the lower box shows a pair of BrdU⁺ migratory neurons (F'').

(G) E12.5 Nkx2.1-Cre;LSL-Tva mouse embryos injected with a mixture of RCAS-GFP and RCAS-mCherry viruses and harvested at P28.

(H) Coronal section of mouse injected with mixed virus showing clusters of red, green, and yellow cells.

(I) Cumulative proportion of nearest neighbor distribution (NND) of same (black) and different (red) fluorophores (n = 3 brains, 215 cells, p < 0.01, Kolmogorov-Smirnov). Scale bars: (B) 50 μm and (G) 100 μm .

positions due to the distances and speed at which they migrated (Movie S1).

To address the possibility that sibling cells may be intrinsically programmed to reach the same cortical destination, we sought a method whereby clonal progeny could be distinguished in the mature cortex. We were able to specifically label MGE progenitors through the combined use of transgenic mice and retroviral

vectors so that only MGE progenitors would be infected. We utilized a genetically modified Replication Competent ASLV long terminal repeat with Splice Acceptor (RCAS) viral vector, combined with transgenic expression of the RCAS cognate receptor TVA in cells of the ganglionic eminence (Figure 2A). Under normal conditions, RCAS vectors are only able to infect avian cells (Young et al., 1993). However, the use of transgenic mice that express the cognate TVA receptor enables the virus to infect mammalian cells (Brown et al., 2011; von Werder et al., 2012). We used two mutant mouse lines to express TVA in

ventral telencephalic progenitors: Olig2-Tva-ires-Cre, in which Tva-ires-Cre is knocked into the Olig2 locus, and Nkx2.1-Cre;LSL-Tva lines (Brown et al., 2011; Schüller et al., 2008; von Werder et al., 2012; Xu et al., 2008) (Figures 2A and S3). We were able to achieve specific and sparse labeling of progenitors in the ganglionic eminences with in utero intraventricular injection of a recombinant GFP-expressing RCAS virus and

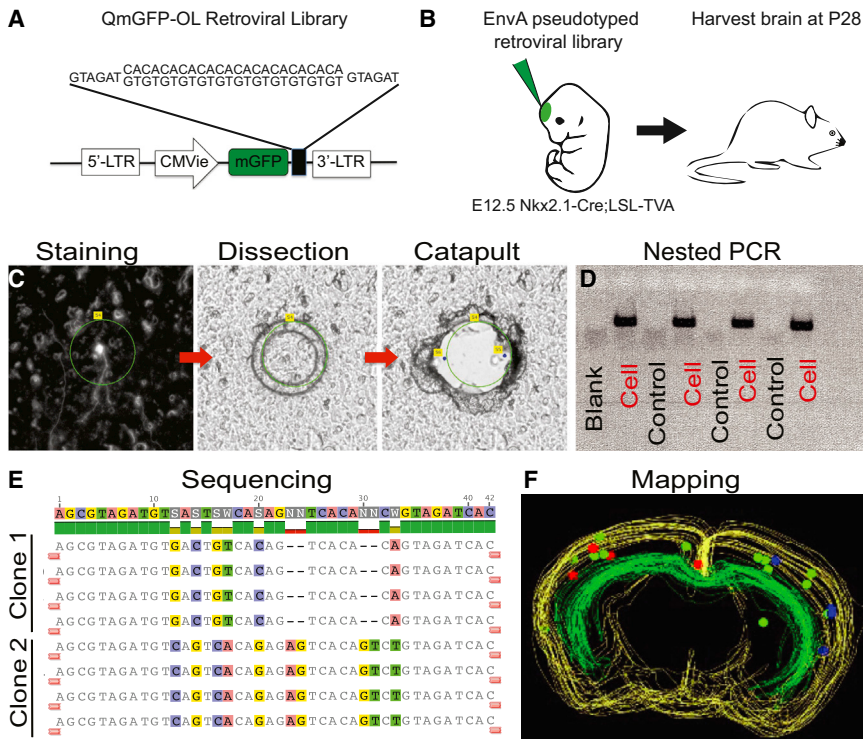


Figure 3. Lineage Analysis of Nkx2.1+ Progenitors Using Barcode Retroviral Library

(A) Schematic of the QmGFP-OL murine retroviral library. Each retrovirus expresses membrane GFP and contains a 24-bp barcode sequence.

(B) EnvA pseudotyped retrovirus libraries were intraventricularly delivered into Nkx2.1-Cre;LSL-Tva embryos at E12.5; brains were harvested and analyzed at P28.

(C) Stained neuron outlined for laser capture microdissection and catapulting.

(D) Example gel of nested PCR products of dissected cells and GFP-negative tissue sections used as controls.

(E) Example barcode sequence alignment showing two four-cell clones with matching barcodes.

(F) 3D map of two four-cell clones shown in red and blue. Green spheres show cells which did not return a barcode sequence.

confirmed that the injection of RCAS into both TVA lines at E12.5 resulted in specific labeling of interneurons in the mature brain (Figures 2B, 2C, and S3). Most GFP-positive cells co-labeled with the interneuron subtype markers PV and SOM (53.0% and 24.0%, respectively; $n = 4$ brains, 701 cells) (Figure 2D). We chose to focus the rest of our analysis on the Nkx2.1-Cre; LSL-Tva line because infection was confined to MGE progenitors instead of all ventral telencephalic progenitors, as in the Olig2-Tva-Cre line (Figures S3A–S3C).

Upon in utero intraventricular injection of RCAS-GFP into E12.5 Nkx2.1-Cre; LSL-Tva mice, we observed clustering of cortical interneurons in both the mature and developing cortex, consistent with previous reports of clustering of sparse virus-labeled neurons (Brown et al., 2011; Ciceri et al., 2013) (Figures 2E and 2F). We reasoned that if sibling cells were clustered, we should observe segregation and/or aggregation of virus-labeled cells derived from a common progenitor. To this end, we injected E12.5 embryos from Nkx2.1-Cre;LSL-Tva mice with a mixture of RCAS-GFP:RCAS-mCherry viruses (Figure 2G). Our rationale was that we would observe clusters of GFP- and mCherry-positive clonally related clusters dispersed throughout the brain. We harvested the injected brains at P28 and found numerous examples of cell clusters consisting of red, green, and yellow cells (Figure 2H). We then measured the cumulative nearest neighbor distribution between cells of the same or different color (Figure 2I). We found that different color neighbors were more closely distributed than cells of the same color ($p < 0.01$, $n = 3$ brains, 234 cells), suggesting that clustering can occur independently of lineage. However, the true distribution of cells in relation to their clonal siblings cannot be determined with this method because clustered cells sharing the same color could be derived from different progenitors.

each virus contained a transgene for membrane-bound GFP. The retroviral library, consisting of 10^5 unique 24-bp barcode sequences, was injected in utero into the lateral ventricle of E12.5 Nkx2.1-Cre;LSL-Tva embryos at a concentration between 5×10^7 and 5×10^5 cfu/ml (Figure 3B). Brains of infected transgenic mice were harvested at P28 and sectioned and stained for interneuron subtype markers PV and SOM. The position of each cell and its histological subtype was then recorded (Table S1). In order to determine the barcode sequence, each mapped cell was collected by laser capture microdissection, and the viral tag was amplified by nested PCR and sequenced (Figures 3C–3E). The clonal, histological, and spatial information was then combined to build 3D maps of GFP-positive cells in the brains of P28 mice (Figure 3F). In order to control for contamination and screen for viral silencing, we randomly collected and PCR-amplified GFP-negative pieces of tissue for every GFP-positive cell. A very small number of barcodes were detected from GFP-negative tissue ($< 1\%$, $n = 701$ cells). Between 14 and 234 cells were labeled from each injection ($n = 8$ hemispheres, 4 brains). Given the number of cells infected in each hemisphere, the probability of neurons containing the same tag arising from two independent progenitor infections is exceedingly low (Cepko et al., 1995; Jiang et al., 2013; Walsh and Cepko, 1992). Therefore, multiple cells sharing the same barcode are presumed to be clonally related siblings.

Amplified and sequenced barcodes were obtained from 302 cells, 30.1% of which were part of a multi-cell clone, defined as two or more cells sharing the same barcode. The majority of individual cells (69.9%) carried unique barcodes, indicating that either they were single cell clones, or we failed to amplify the barcode of their sibling cells. The average size of multi-cell

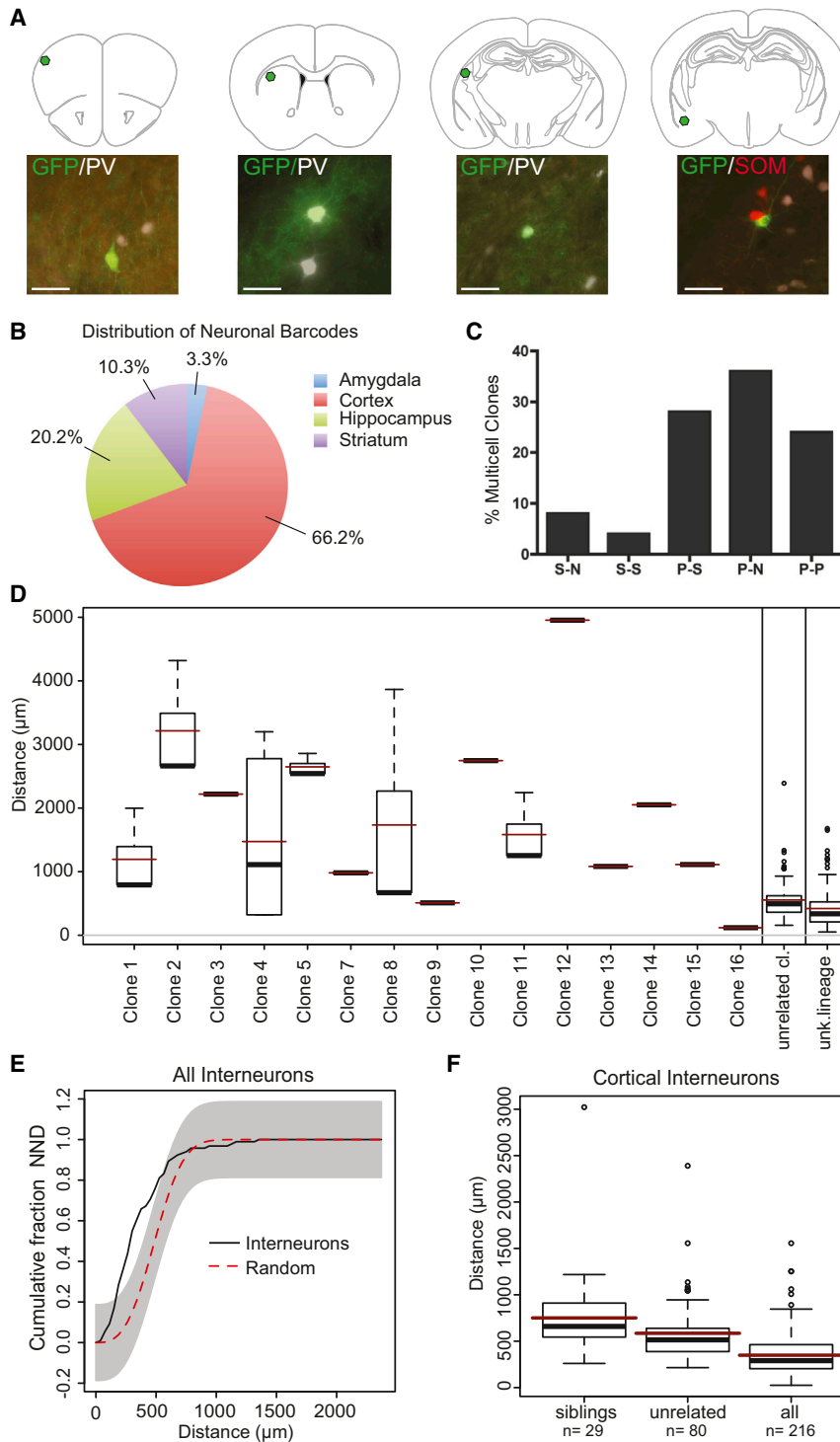


Figure 4. Interneuron Clones Consist of Widely Dispersed Cells of Diverse Subtypes

(A) Representative schematic of a four-cell clone containing three PV cells (white) and one SOM cell (red) dispersed across thousands of microns in the brain.

(B) Pie chart of forebrain regions that contain neurons that returned a barcode in Nkx2.1-Cre;LSL-Tva virus-injected mice ($n = 302$ cells).

(C) Bar graph showing the proportion of multi-cell clones composed of at least one cell type. S: somatostatin, P: parvalbumin, and N: negative for both markers ($n = 84$ cells, 26 clones).

(D) Box plot representing all of the NNDs between pairs of cells in each clone. The marks in the boxes are the 1st, 2nd (median), and 3rd quartile of the distances, with the dots representing the outliers. Superimposed red lines represent the mean distances in each group, and black bars represent the median distances ($n = 2$ brain hemispheres, 284 cells).

(E) Cumulative (NND) of Nkx2.1-Cre;LSL-Tva brains ($n = 284$), 500. The grey band shown in the plot is the 95% confidence band based on 500 simulated occurrences of complete spatial random events.

(F) Box plot representing NND of cortical interneurons. Sibling clones are significantly more widely distributed than unrelated cortical neurons, and all neurons (both with and without tags) (multi-versus single $p < 0.01$; multi versus all $p < 0.001$, Kruskal-Wallis test) Scale bar: 50 μm .

clones was 2.8 cells, with the largest clones containing six cells (Figure 4A). Neurons that returned barcode sequence tags were widely dispersed across multiple forebrain structures including the amygdala, cortex, hippocampus, and striatum, with the majority located in the cortex (66.2%, $n = 302$) (Figure 4B). We never observed clonal siblings in different hemispheres or mixed

clones consisting of neurons and glia (data not shown). When we examined the composition of multi-cell clones, we found that nearly 30% consisted of a mixture of PV and SOM subtypes, while fewer than 30% were positive for a single marker, and 20% were negative for both markers (Figures 4A and 4C). We were unable to discern a predominant composition of mixed subtype clones, as we observed clones with either PV⁺ or SOM⁺ cells as a major component (Figures 4A, S5A, and S5B).

When examining the spatial distribution of multi-cell clones, we observed that sibling neurons were widely dispersed across different brain structures. Most cells were located hundreds or thousands of microns from their nearest identified sibling cell (Figures 4A and 4D). The only observed pair of clonally related cells located in the same 25- μm thick brain section

was a pair of glia in the septum, consistent with previous findings of local proliferation of glial progenitor cells (Figure 4D, Clone 16) (Ge et al., 2012). We examined the nearest neighbor distribution of retrovirus-labeled GFP-positive cells by assigning coordinates to each cell during serial section reconstruction and categorizing cells as sibling members of a multi-cell clone,

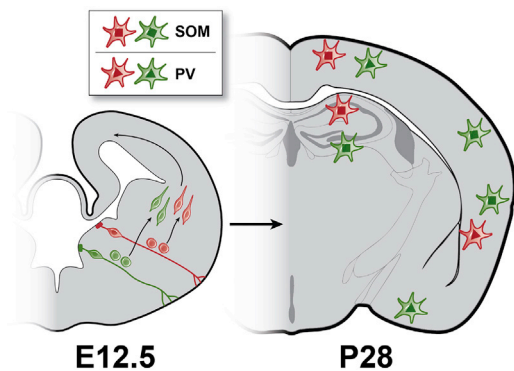


Figure 5. Wide Dispersion and Diversity of Clonally Related Interneurons

Left: Coronal section of embryonic (E12.5) mouse brain illustrating distinct clonal lineages of MGE progenitors (red and green). Radial glia must divide asymmetrically to produce intermediate progenitor cells, which divide symmetrically to produce pairs of newborn interneurons. The newborn neurons must then migrate tangentially to reach their final destinations in the forebrain. Right: Postnatal day (P28) mouse brain illustrating clones composed of SOM and PV subtypes dispersed widely across different functional and structural regions of the cortex, striatum (not shown) and hippocampus.

unrelated clones, or cells that did not return a barcode sequence (unknown lineage) (Figure 4D; Table S1). The average distance between siblings was substantially larger than that of unrelated clones. A substantial portion of multi-cell cortical clones had at least one sibling cell located in a different forebrain structure (42.1%, $n = 3$ brains), while the remainder of clones were confined to the cortex. We plotted the NND of all cells, regardless of category, and compared them to 500 computer simulations of randomly distributed neurons (Figure 4E). We found that between approximately 250–500 μm in NND there were significant differences in the spatial organization of our experimental dataset when compared to randomized simulations ($n = 284$ cells), suggesting that the overall population distribution is not random, consistent with previous studies (Brown et al., 2011). Next, we compared the NND of cortical sibling clones to unrelated cortical clones. We found the NND of cortical sibling clones to have a significantly wider dispersion than unrelated clones (mean 750 μm versus 585 μm , respectively; $p = 0.01$, $n = 2$ hemispheres, 216 cells) (Figure 4E), suggesting that more closely clustered cells are derived from independent clonal lineages. Taken together, our findings suggest that MGE interneurons derived from a common progenitor are widely dispersed across different regions of the brain and that the majority of clustered cells observed with sparse viral labeling are likely not clonally related.

DISCUSSION

Using retroviral fate mapping and genetic tagging, we followed the development of cortical interneurons to understand the role of clonal relationships in regulating their integration into functional circuitry. Ventral telencephalic RG appear to be the primary neural stem cells, dividing asymmetrically to produce IPCs that subsequently divide symmetrically to expand their numbers, or more frequently, to produce pairs of neurons. These

findings suggest significant similarities in the patterns of cell division in the dorsal and ventral regions of the telencephalon. However, there are possible differences in cell cycle dynamics, proliferative potential, and relative proportions of progenitor subtypes that likely lead to differences in SVZ organization and the number of cells produced in each region (Pilz et al., 2013). The developmental history of clonally related cells in the cortex and MGE diverges significantly once postmitotic neurons are produced. Newborn excitatory neurons derived from the same clonal lineage in the cortex migrate along RG and generally remain closely associated. These neurons remain vertically aligned in the developing rodent brain, allowing them to have continuous contact with their siblings (Noctor et al., 2001). In contrast, newborn inhibitory interneurons are highly motile and do not appear to maintain an association with their sibling cells. The long distances inhibitory neurons must migrate to reach their target region may preclude the development of sustained connectivity between related cells, which may necessitate alternative strategies for circuit organization independent of lineage relationships.

Dispersion of Clonally Related Interneurons

There has been significant interest in the role that clonal relationships might play in the organization of cortical neurons. It has been previously suggested that clonal identity could influence the connectivity of sibling cells within cortical circuits (Li et al., 2012; Sultan et al., 2014; Yu et al., 2012). The clustered appearance of radially and horizontally aligned interneurons following sparse viral labeling is visually striking and appears to support the idea that clonal relationships dictate these alignments (Brown et al., 2011; Ciceri et al., 2013). However, we consistently found that interneuron clones were widely dispersed throughout different forebrain regions and that clustered cells were clonally distinct, suggesting that interneuron clusters observed following sparse retroviral labeling are largely composed of unrelated cells (Figure 5). What are the possible reasons for the discrepancy between our interpretation and those of previous studies? The key methodological difference is our use of large numbers of tags to differentiate cells derived from separate clonal lineages. Utilizing a sufficiently complex library of tags is necessary to prevent erroneous assignment of clonal relationships between cells based only on their proximity. This is especially important when tracing the lineage of cells with a broad migratory capacity such as those derived from the MGE. Two previous studies utilized either one or two markers to differentiate cells of different lineages, and it is worth noting that even when utilizing two fluorescent tags for sparse labeling, Ciceri et al. (2013) observed mixing of the two labels in over half of their clusters.

Technical Considerations for Lineage Tracing with Barcodes

Retroviral barcode libraries provide a powerful method for determining lineage relationships in populations of cells regardless of their pattern of migration, but this method has limitations related to gene silencing and cell death. Silencing of the retroviral reporter may be a factor contributing to the small clone size we observed in our analysis. We attempted to survey for silencing by random laser-capture microdissection of GFP-negative tissue.

However, given the wide dispersion of clonal cells, our random cell collections likely yielded an underestimate of silencing. A study using the same retroviral reporter used here and systematically examining silencing across large areas of GFP-negative brain tissue found that silencing can account for some reduction in clone size, but notably did not uncover a consistent pattern of silencing (Mayer et al., 2015). Consistent with previous studies using retroviral barcode libraries, we recovered tags from only a portion of labeled cells—43% of GFP-positive cells (302 out of 701)—a limitation that can also affect determination of clone size and composition (Reid and Walsh, 2002). While these factors prevent us from drawing conclusions about the true size of the clones or their complete pattern of composition, we do not believe this affects our interpretation. To our knowledge, retroviral silencing is a random event, so if sibling clustering were a dominant mechanism for organization, we would expect some portion of our multi-cell clones to be clustered. However, nearly all of our clonally related cells were widely dispersed, and we observed clustering of unrelated cells. As mentioned above, we sampled a piece of GFP-negative tissue for every cell collected typically within the same field of view as the GFP-positive cell. On the rare occasions when we amplified tags from GFP-negative tissue, the barcode never matched the GFP-positive cell that was nearby. Our findings support the idea that clonal lineage is not the primary determinant for spatial aggregation of MGE-derived interneurons. Our data also suggest that spatial and temporal origin may influence clustering. Nonetheless, we cannot rule out the possibility that a small subpopulation of clonally related cells could be clustered.

In our study, we focused on the distribution of clones in the P28 mouse brain, past the period of cortical interneuron cell death (Southwell et al., 2012). It is therefore possible that intrinsically determined cell death could play a role in regulating the distribution and composition of interneuron clones. However, it seems unlikely that the pattern of apoptosis has significantly distorted our observed clonal relationships, since similar clusters of sparse retroviral labeled interneurons have been observed both before and after the peak period of cell death (Brown et al., 2011; Ciceri et al., 2013). The demonstration that clusters include unrelated cells indicates that a mechanism other than lineage contributes to clustering, regardless of a possible role of cell death.

Spatial and Temporal Regulation of Neuronal Organization

How can independently generated, non-related neurons arrive at the same cortical site? One possibility is that the spatial and temporal origin of interneurons might play an instructive role in determining their final position (Ciceri et al., 2013; Marín and Müller, 2014). This possibility raises the question of whether spatial and temporal identities might also dictate circuit relationships between cortical interneurons.

While functionally and histologically distinct PV and SOM interneuron subtypes are both derived from the MGE (Kepecs and Fishell, 2014), it has been unclear whether they derive from distinct or common progenitor lineages. Our observation that the majority of multi-cell clones consisted of both SOM and PV subtypes suggests that at E12.5 single MGE progenitors

generate multiple neuronal subtypes. This has important implications for understanding the cellular mechanisms regulating cell fate determination. Distinct neuronal subtypes might be generated within a single clone in a specific temporal pattern. A temporal pattern of neural subtype production occurs in invertebrates and also in clones of excitatory neurons where deep layer subcortical projection neurons are produced first, followed by superficial layer callosal projection neurons (Bayraktar and Doe, 2013; Kohwi and Doe, 2013; Leone et al., 2008). Alternatively, two sibling cells sharing the same birthdate could have different cell fates, as has been shown in the retina where intermediate progenitors produce two daughter cells with distinct postmitotic cell fates (Cepko, 2014). IPCs in the MGE could similarly generate daughter cells of different subtypes. Further studies will be necessary to determine the subtype identity of the daughters of IPC divisions in the MGE.

EXPERIMENTAL PROCEDURES

Retrovirus Production and In Utero Injections

Replication-incompetent GFP-expressing retrovirus was produced from a stably transfected packaging line and injected into E12.5 gestation stage pregnant mice, as previously reported (Noctor et al., 2001).

Immunostaining and Laser-Microdissection Microscopy

Mice were sacrificed and their brains were processed for immunohistochemistry as previously described. Floating sections (25 μm) were stained with the following primary antibodies: chicken anti-GFP (1:750, Aves Lab) rabbit anti-somatostatin (Millipore, 1:750); mouse anti-parvalbumin (Millipore 1:1000). Secondary antibodies used were Alexafluor 488 (1:1,000), 546 (1:500), or 647 (1:500) conjugated donkey anti-mouse, anti-rabbit, or anti-goat (Life Technologies). Sections were mounted in PEN-membrane slides (2 μm , JH Technologies). Individual labeled cells were mapped and laser microdissected with a small amount of surrounding tissue (4,000–6,000 μm^2) using a Zeiss PALM MicroBeam LCM (v4.3.2.13, Carl Zeiss MicroImaging). GFP-negative control tissue was also dissected for every positive dissection. Dissected tissue was collected in 20 μl of Proteinase K solution (20 $\mu\text{g}/\text{ml}$ proteinase K [Roche], 50 mM TrisHCl [pH 7.5], 50 mM KCl, 2.5 mM MgCl_2 , and 0.5% Igepal CA-630 [Sigma]) and incubated for 2 hr at 60°C, followed by 20 min at 85°C and 10 min at 95°C. The first round of PCR “barcode” amplification was done by adding 40 μl of 1st PCR mix that included Platinum Pfx DNA Polymerase (Life Technologies) and primers SBR161 (5'-GACAACCACTACTGAGCA CCCAGT-3') and SBR126 (5'-GGCTCGTACTCTATAGCTTCAGCTGGTGA-3'). The 2nd PCR mix included 2 μl of the 1st PCR reaction, Platinum Pfx DNA Polymerase, and primers SBR160 (5'-ATCACATGGTCCCTGGAGTTC GTGA-3') and SBR128 (5'-ATTGTTGAGTCAAACTAGAGCCTGGACCA-3') to a total of 20 μl . PCR products were cleaned and sequenced using primer SB160. After identification of clones, the positions of selected positive cells were reconstructed in 3D images using NeuroLucida (v10.31 MBF Biosciences-MicroBrightField Inc.).

Brain Sectioning, Cortical Slice Culture, Viral Infection on Slice, and Time-Lapse Imaging

Retrovirus infected brains were vibratome-sliced, cultured, and imaged as previously described (Noctor et al., 2001).

Statistical Analysis

GFP-positive cells were assigned coordinates from serial section reconstructions using NeuroLucida. After determining the distance between each interneuron and its closest labeled neighbor, we compared these distances to the values expected for a sample of neurons located at random in the same volume. Specifically, for each experiment, the experimental interneuron distribution was compared with 100 simulated distributions, generated by positioning the same number of elements at random locations distributed uniformly

in the exact same region of tissue as the experimental condition. NNDs were displayed as cumulative distributions.

SUPPLEMENTAL INFORMATION

Supplemental Information includes five figures, one table, one movie, and Supplemental Experimental Procedures and can be found with this article online at <http://dx.doi.org/10.1016/j.neuron.2015.07.030>.

AUTHOR CONTRIBUTIONS

C.C.H., L.C.F., A.A.-B., and A.R.K. designed research; C.C.H., L.C.F., A.G.-C., P.R.L.P., C.C.G., and M.T.G. conducted experiments. C.L.C. developed the EnvA pseudotyped retroviral library and critically reviewed and edited the manuscript. C.C.H. and E.M. analyzed data. C.C.H. and A.R.K. wrote the manuscript.

ACKNOWLEDGMENTS

We would like to thank William Walantus and Yingying Wang for technical assistance with in utero viral injections and histology. We thank members of the Alvarez-Buylla, Rowitch and Kriegstein labs for ideas arising from numerous critical discussions. We are extremely grateful to Rebecca Ihrle for providing brain atlas tracings. This project was supported by NIH R01NS035710 to A.R.K. and NIH R37HD032116 to A.A.-B. and HHMI to C.L.C.

Received: March 10, 2015

Revised: May 28, 2015

Accepted: July 27, 2015

Published: August 20, 2015

REFERENCES

- Anderson, S.A., Marín, O., Horn, C., Jennings, K., and Rubenstein, J.L. (2001). Distinct cortical migrations from the medial and lateral ganglionic eminences. *Development* *128*, 353–363.
- Anderson, S.A., Kaznowski, C.E., Horn, C., Rubenstein, J.L., and McConnell, S.K. (2002). Distinct origins of neocortical projection neurons and interneurons in vivo. *Cereb. Cortex* *12*, 702–709.
- Bayraktar, O.A., and Doe, C.Q. (2013). Combinatorial temporal patterning in progenitors expands neural diversity. *Nature* *498*, 449–455.
- Brown, K.N., Chen, S., Han, Z., Lu, C.-H., Tan, X., Zhang, X.-J., Ding, L., Lopez-Cruz, A., Saur, D., Anderson, S.A., et al. (2011). Clonal production and organization of inhibitory interneurons in the neocortex. *Science* *334*, 480–486.
- Butt, S.J.B., Fuccillo, M., Nery, S., Noctor, S., Kriegstein, A., Corbin, J.G., and Fishell, G. (2005). The temporal and spatial origins of cortical interneurons predict their physiological subtype. *Neuron* *48*, 591–604.
- Butt, S.J., Sousa, V.H., Fuccillo, M.V., Hjerling-Leffler, J., Miyoshi, G., Kimura, S., and Fishell, G. (2008). The requirement of Nkx2-1 in the temporal specification of cortical interneuron subtypes. *Neuron* *59*, 722–732.
- Casarosa, S., Fode, C., and Guillemot, F. (1999). Mash1 regulates neurogenesis in the ventral telencephalon. *Development* *126*, 525–534.
- Cepko, C. (2014). Intrinsically different retinal progenitor cells produce specific types of progeny. *Nat. Rev. Neurosci.* *15*, 615–627.
- Cepko, C., Ryder, E.F., Austin, C.P., Walsh, C., and Fekete, D.M. (1995). Lineage analysis using retrovirus vectors. *Methods Enzymol.* *254*, 387–419.
- Ciceri, G., Dehorter, N., Sols, I., Huang, Z.J., Maravall, M., and Marín, O. (2013). Lineage-specific laminar organization of cortical GABAergic interneurons. *Nat. Neurosci.* *16*, 1199–1210.
- Fuentealba, L.C., Rompani, S.B., Parraguez, J.I., Obernier, K., Romero, R., Cepko, C.L., and Alvarez-Buylla, A. (2015). Embryonic Origin of Postnatal Neural Stem Cells. *Cell* *161*, 1644–1655.
- Ge, W.P., Miyawaki, A., Gage, F.H., Jan, Y.N., and Jan, L.Y. (2012). Local generation of glia is a major astrocyte source in postnatal cortex. *Nature* *484*, 376–380.
- Hansen, D.V., Lui, J.H., Parker, P.R., and Kriegstein, A.R. (2010). Neurogenic radial glia in the outer subventricular zone of human neocortex. *Nature* *464*, 554–561.
- Haubensak, W., Attardo, A., Denk, W., and Huttner, W.B. (2004). Neurons arise in the basal neuroepithelium of the early mammalian telencephalon: a major site of neurogenesis. *Proc. Natl. Acad. Sci. USA* *101*, 3196–3201.
- Jiang, H., Wang, L., Beier, K.T., Cepko, C.L., Fekete, D.M., and Brigande, J.V. (2013). Lineage analysis of the late otocyst stage mouse inner ear by transuterine microinjection of a retroviral vector encoding alkaline phosphatase and an oligonucleotide library. *PLoS ONE* *8*, e69314.
- Kepecs, A., and Fishell, G. (2014). Interneuron cell types are fit to function. *Nature* *505*, 318–326.
- Kohwi, M., and Doe, C.Q. (2013). Temporal fate specification and neural progenitor competence during development. *Nat. Rev. Neurosci.* *14*, 823–838.
- Leone, D.P., Srinivasan, K., Chen, B., Alcamo, E., and McConnell, S.K. (2008). The determination of projection neuron identity in the developing cerebral cortex. *Curr. Opin. Neurobiol.* *18*, 28–35.
- Li, Y., Lu, H., Cheng, P.L., Ge, S., Xu, H., Shi, S.H., and Dan, Y. (2012). Clonally related visual cortical neurons show similar stimulus feature selectivity. *Nature* *486*, 118–121.
- Lui, J.H., Hansen, D.V., and Kriegstein, A.R. (2011). Development and evolution of the human neocortex. *Cell* *146*, 18–36.
- Marín, O. (2013). Cellular and molecular mechanisms controlling the migration of neocortical interneurons. *Eur. J. Neurosci.* *38*, 2019–2029.
- Marín, O., and Müller, U. (2014). Lineage origins of GABAergic versus glutamatergic neurons in the neocortex. *Curr. Opin. Neurobiol.* *26*, 132–141.
- Mayer, C., Jaglin, X.H., Cobbs, L.V., Bandler, R.C., Streicher, C., Cepko, C.L., Hippenmeyer, S., and Fishell, G. (2015). Clonally related forebrain interneurons disperse broadly across both functional areas and structural boundaries. *Neuron* *87*, this issue, 989–998.
- Miller, F.D., and Gauthier, A.S. (2007). Timing is everything: making neurons versus glia in the developing cortex. *Neuron* *54*, 357–369.
- Miyoshi, G., Butt, S.J.B., Takebayashi, H., and Fishell, G. (2007). Physiologically distinct temporal cohorts of cortical interneurons arise from telencephalic Olig2-expressing precursors. *J. Neurosci.* *27*, 7786–7798.
- Nery, S., Fishell, G., and Corbin, J.G. (2002). The caudal ganglionic eminence is a source of distinct cortical and subcortical cell populations. *Nat. Neurosci.* *5*, 1279–1287.
- Nóbrega-Pereira, S., Kessar, N., Du, T., Kimura, S., Anderson, S.A., and Marín, O. (2008). Postmitotic Nkx2-1 controls the migration of telencephalic interneurons by direct repression of guidance receptors. *Neuron* *59*, 733–745.
- Noctor, S.C., Flint, A.C., Weissman, T.A., Dammerman, R.S., and Kriegstein, A.R. (2001). Neurons derived from radial glial cells establish radial units in neocortex. *Nature* *409*, 714–720.
- Noctor, S.C., Martínez-Cerdeño, V., Ivic, L., and Kriegstein, A.R. (2004). Cortical neurons arise in symmetric and asymmetric division zones and migrate through specific phases. *Nat. Neurosci.* *7*, 136–144.
- Petryniak, M.A., Potter, G.B., Rowitch, D.H., and Rubenstein, J.L.R. (2007). Dlx1 and Dlx2 control neuronal versus oligodendroglial cell fate acquisition in the developing forebrain. *Neuron* *55*, 417–433.
- Pilz, G.A., Shitamukai, A., Reillo, I., Pacary, E., Schwausch, J., Stahl, R., Ninkovic, J., Snippert, H.J., Clevers, H., Godinho, L., et al. (2013). Amplification of progenitors in the mammalian telencephalon includes a new radial glial cell type. *Nat. Commun.* *4*, 2125.
- Rakic, P. (1988). Specification of cerebral cortical areas. *Science* *241*, 170–176.

- Reid, C.B., and Walsh, C.A. (2002). Evidence of common progenitors and patterns of dispersion in rat striatum and cerebral cortex. *J. Neurosci.* *22*, 4002–4014.
- Schüller, U., Heine, V.M., Mao, J., Kho, A.T., Dillon, A.K., Han, Y.G., Huillard, E., Sun, T., Ligon, A.H., Qian, Y., et al. (2008). Acquisition of granule neuron precursor identity is a critical determinant of progenitor cell competence to form Shh-induced medulloblastoma. *Cancer Cell* *14*, 123–134.
- Southwell, D.G., Paredes, M.F., Galvao, R.P., Jones, D.L., Froemke, R.C., Sebe, J.Y., Alfaro-Cervello, C., Tang, Y., Garcia-Verdugo, J.M., Rubenstein, J.L., et al. (2012). Intrinsically determined cell death of developing cortical interneurons. *Nature* *491*, 109–113.
- Sultan, K.T., Shi, W., and Shi, S.H. (2014). Clonal origins of neocortical interneurons. *Curr. Opin. Neurobiol.* *26*, 125–131.
- Tanaka, D.H., Yanagida, M., Zhu, Y., Mikami, S., Nagasawa, T., Miyazaki, J., Yanagawa, Y., Obata, K., and Murakami, F. (2009). Random walk behavior of migrating cortical interneurons in the marginal zone: time-lapse analysis in flat-mount cortex. *J. Neurosci.* *29*, 1300–1311.
- Tricoire, L., Pelkey, K.A., Erkkila, B.E., Jeffries, B.W., Yuan, X., and McBain, C.J. (2011). A blueprint for the spatiotemporal origins of mouse hippocampal interneuron diversity. *J. Neurosci.* *31*, 10948–10970.
- Vasistha, N.A., Garcia-Moreno, F., Arora, S., Cheung, A.F., Arnold, S.J., Robertson, E.J., and Molnar, Z. (2014). Cortical and Clonal Contribution of Tbr2 Expressing Progenitors in the Developing Mouse Brain. *Cerebral cortex*.
- von Werder, A., Seidler, B., Schmid, R.M., Schneider, G., and Saur, D. (2012). Production of avian retroviruses and tissue-specific somatic retroviral gene transfer in vivo using the RCAS/TVA system. *Nat. Protoc.* *7*, 1167–1183.
- Walantus, W., Castaneda, D., Elias, L., and Kriegstein, A. (2007). In utero intraventricular injection and electroporation of E15 mouse embryos. *J. Vis. Exp.* *239*, <http://dx.doi.org/10.3791/239>.
- Walsh, C., and Cepko, C.L. (1992). Widespread dispersion of neuronal clones across functional regions of the cerebral cortex. *Science* *255*, 434–440.
- Wang, X., Tsai, J.W., LaMonica, B., and Kriegstein, A.R. (2011). A new subtype of progenitor cell in the mouse embryonic neocortex. *Nat. Neurosci.* *14*, 555–561.
- Wonders, C.P., and Anderson, S.A. (2006). The origin and specification of cortical interneurons. *Nat. Rev. Neurosci.* *7*, 687–696.
- Xu, Q., Cobos, I., De La Cruz, E., Rubenstein, J.L., and Anderson, S.A. (2004). Origins of cortical interneuron subtypes. *J. Neurosci.* *24*, 2612–2622.
- Xu, Q., Tam, M., and Anderson, S.A. (2008). Fate mapping Nkx2.1-lineage cells in the mouse telencephalon. *J. Comp. Neurol.* *506*, 16–29.
- Young, J.A., Bates, P., and Varmus, H.E. (1993). Isolation of a chicken gene that confers susceptibility to infection by subgroup A avian leukosis and sarcoma viruses. *J. Virol.* *67*, 1811–1816.
- Yu, Y.-C., Bultje, R.S., Wang, X., and Shi, S.-H. (2009). Specific synapses develop preferentially among sister excitatory neurons in the neocortex. *Nature* *458*, 501–504.
- Yu, Y.C., He, S., Chen, S., Fu, Y., Brown, K.N., Yao, X.H., Ma, J., Gao, K.P., Sosinsky, G.E., Huang, K., and Shi, S.H. (2012). Preferential electrical coupling regulates neocortical lineage-dependent microcircuit assembly. *Nature* *486*, 113–117.